Hindawi Publishing Corporation
Advances in Acoustics and Vibration
Volume 2010, Article ID 730813, 9 pages
doi:10.1155/2010/730813

Research Article

A Control Source Structure of Single Loudspeaker and Rear Sound Interference for Inexpensive Active Noise Control

Yasuhide Kobayashi,[1] Hisaya Fujioka,[2] and Naoki Jinbo[3]

[1] *Department of Mechanical Engineering, Faculty of Engineering, Nagaoka University of Technology, Nagaoka, Niigata 940-2188, Japan*
[2] *Department of Applied Analysis and Complex Dynamical Systems, Graduate School of Informatics, Kyoto University, Kyoto 606-8501, Japan*
[3] *Graduate School of Engineering, Nagaoka University of Technology, Niigata 940-2188, Japan*

Correspondence should be addressed to Yasuhide Kobayashi, kobayasi@vos.nagaokaut.ac.jp

Received 17 March 2010; Accepted 4 June 2010

Academic Editor: Marek Pawelczyk

Copyright © 2010 Yasuhide Kobayashi et al. This is an open access article distributed under the Creative Commons Attribution License, which permits unrestricted use, distribution, and reproduction in any medium, provided the original work is properly cited.

Active noise control systems of simple ducts are investigated. In particular, open-loop characteristics and closed-loop performances corresponding to various structures of control sources are compared based on both mathematical models and experimental results. In addition to the standard single loudspeaker and the Swinbanks' source, we propose and examine a single loudspeaker with a rear sound interference as a novel structure of control source, where the rear sound radiated from the loudspeaker is interfered with the front sound in order to reduce the net upstream sound directly radiated from the control source. The comparisons of the control structures are performed as follows. First, the open-loop transfer function is derived based on the standard wave equation, where a generalized control structure unifying the three structures mentioned above is considered. Secondly, by a comparison of the open-loop transfer functions from the first principle modeling and frequency response experiments, it is shown that a certain phase-lag is imposed by the Swinbanks' source and the rear sound interference. Thirdly, effects on control performances of control source structures are examined by control experiments with robust controllers.

1. Introduction

It is well known that the Swinbanks' (unidirectional) source [1] has advantages against a standard single loudspeaker (bidirectional source) in not only performances but also the implementation cost. Indeed, the performance improvement has been reported experimentally in both adaptive and robust control setups [2, 3]. In addition, the possibility of inexpensive implementation has been pointed out by showing that the controller gain is lower and, as the result, lower amplitude of driving signal for loudspeakers are achieved by the Swinbanks' source [2, 4], which enables us to use lower power loudspeakers. Furthermore, it has been shown that the advantages of Swinbanks' source are theoretically proved for a practical setting on the duct length and loudspeaker locations [5, 6].

The Swinbanks' source is composed of two loudspeakers where the upstream sound radiated directly from the downstream loudspeaker is cancelled out by the sound with the same amplitude and the opposite phase generated by the upstream loudspeaker. The advantage of the Swinbanks' source are mainly obtained by the extension of the time period by which the upstream sound directly radiated from the control source travels to the reference microphone. Indeed, it is empirically known that the closed-loop performance is improved when the actuator (control source) and the sensor (reference microphone) are well separated in space [7, 8].

The reverse-phased sound in the Swinbanks' source is, however, also radiated from the backside of the loudspeakers while it is not utilized in the existing control source for active noise control (ANC). Therefore, one can expect that a single loudspeaker can achieve a similar performance to the Swinbanks' source if the rear sound could be interfered to reduce the front sound at an upstream junction through some additional ducts. In this scenario, inexpensive

implementation is also expected since the additional loudspeaker in the Swinbanks' source is not necessary to generate opposite-phased sound. Moreover, there is no guarantee that the Swinbanks' source is the best structure for an inexpensive ANC system.

In this paper, we propose a new structure of control source which is composed of a single loudspeaker with a rear sound interference so that the rear sound radiated from the loudspeaker is interfered with the front sound in order to reduce the net upstream sound directly radiated from the control source. The validity of the proposed method will be shown by comparing to the existing two structures of control sources, namely, the standard single loudspeaker (bidirectional source) and the Swinbanks' (unidirectional) source, in terms of the open-loop characteristic and the closed-loop performances based on both mathematical models and experimental results.

2. Experimental Apparatus

Figure 1 and Table 1, respectively, show a block diagram and instruments of the experimental apparatus which are similar to that in [2] except that a real ventilation fan is replaced to a loudspeaker (SPK1) as a noise source, and the duct length is shortened to simplify mathematical models. Two loudspeakers, SPK2 and SPK3, are used as control sources.

In Figure 1, blue lines show PVC pipes of 10 cm in diameter and 7 mm in thickness, while brown thinner lines show flexible PVC ducts which are commercial products for residential ventilation systems and are connected to adjust the duct length. The brown broken curve duct, which is called subduct and is also made by the flexible PVC duct, is used only for the proposed control source after removing SPK3. The experimental apparatus is used in three ways as follows for each structure of the control source:

Case (a). Bidirectional source: SPK3 is turned off, that is, the driving signal $v(t)$ is set to 0. The control source is called bidirectional source in this paper, since the source generates same sounds in upstream and downstream direction.

Case (b). Swinbanks' source [4]: SPK3 is driven to cancel out the upstream sound generated by SPK2, that is, $v(t) = -u(t-\tau)$, $\tau = (l_u - l_v)/c_0$, where $u(t)$ is the driving signal for SPK2, c_0 is the sound speed, and $l_u - l_v$ is the distance between SPK2 and SPK3.

Case (c). Rear-sound-aided source (Proposed source): SPK3 is removed and the subduct is attached so that the rear sound of SPK2 is interfered with the front sound at the junction of ducts. Note that only SPK2 is used and hence the implementation is less expensive than case (b).

The delay τ in the case (b) is approximately implemented as a module of the real-time application interface (RTAI) for Linux that updates the signal $v(t)$ at every 0.1 ms which should be short enough to avoid an aliasing effect. In addition, we use $\tau = 2$ ms which exactly corresponds to 20 times of the period of the real-time module. The effective frequency range of the Swinbanks' source is given as $[f_0, 5f_0] \simeq [40, 200]$ where $f_0 := c_0/(12(l_u - l_v))$ [4], while $c_0 = 344$ m/s in a normal temperature environment. Moreover, the length of the subduct (88 cm) was adjusted experimentally so that the upstream sound cancellation is improved: We can identify the length of the delay by injecting an impulse signal to SPK2 and observing the reference microphone output y. The delay was maximized by adjusting the length of the subduct.

The whole system from $\begin{bmatrix} w \\ u \end{bmatrix}$ to $\begin{bmatrix} z \\ y \end{bmatrix}$ including dynamics of electrical circuits, acoustic ducts, microphones, and loudspeakers, is considered as the plant transfer function $G(s) := \begin{bmatrix} G_{zw}(s) & G_{zu}(s) \\ G_{yw}(s) & G_{yu}(s) \end{bmatrix}$, for each case, where w is the driving signal for SPK1, z is the error microphone signal, and y is the reference microphone signal as depicted in Figure 1. $G(s)$ is used for robust controller design in Section 5. Note that v is determined by u, and hence $G(s)$ depends on the control structure. We will determine $G(s)$ by frequency response experiments, and the experimental results will be compared with the first principle model in the following sections in order to examine the effect of control sources on open-loop characteristics.

3. First Principle Model

In this section, frequency response functions for $G(s)$ defined in the previous section are derived by the first principle modeling where a generalized control structure unifying the three structures previously mentioned is considered. Figure 2 shows a model of $G(s)$. The system is mainly composed of a duct of length L, where a noise source SPK1, a reference microphone, a subduct, a control source SPK2, and an error microphone are located at $x = 0, l_y, l_v, l_u$, and l_z, respectively. The subduct is L_S in length, and is terminated with another control source. $H(s)$ is a transfer function relating two control sources. The control source in Figure 2 gives a general representation including the three control sources as special cases: Case (a) corresponds to $L_S = 0$ and $H(s) = 0$; Case (b) corresponds to $L_S = 0$ and $H(s) = -e^{-s((l_u - l_v)/c_0)}$; Case (c) corresponds to $L_S = l_u - l_v$ and $H(s) = -1$.

In order to derive frequency response functions, let $p_\bullet$ and $u_\bullet$ denote the complex pressure and the particle velocity, respectively, for each position as shown in Figure 2. In addition, dynamics of loudspeakers, microphones, and electrical circuits such as low pass filters, are neglected, since those dynamics have only common contribution to the frequency response functions to be compared for cases (a), (b), and (c). Thus, let us assume for simplicity, that microphone signal is proportional to the complex pressure, and that the complex particle velocity at each loudspeaker is proportional to the driving signal, since our interest is in proportion of the gain and phase characteristics. Specifically, we assume $y = p_y$, $z = p_z$, $u_f = u$, and $u_0 = w$. Then, frequency response functions to be derived are given by $\widetilde{G}(j\omega) := \begin{bmatrix} \widetilde{G}_{zw}(j\omega) & \widetilde{G}_{zu}(j\omega) \\ \widetilde{G}_{yw}(j\omega) & \widetilde{G}_{yu}(j\omega) \end{bmatrix} = \begin{bmatrix} p_z(j\omega)/u_0(j\omega) & p_z(j\omega)/u_f(j\omega) \\ p_y(j\omega)/u_0(j\omega) & p_y(j\omega)/u_f(j\omega) \end{bmatrix}$.

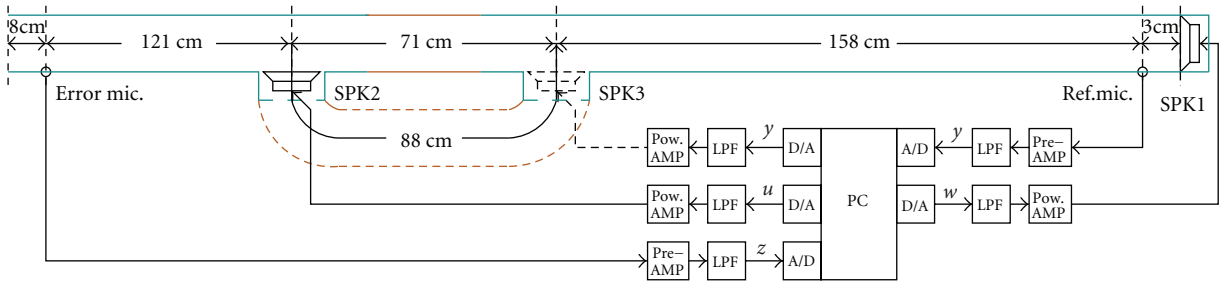

Figure 1: Experimental apparatus.

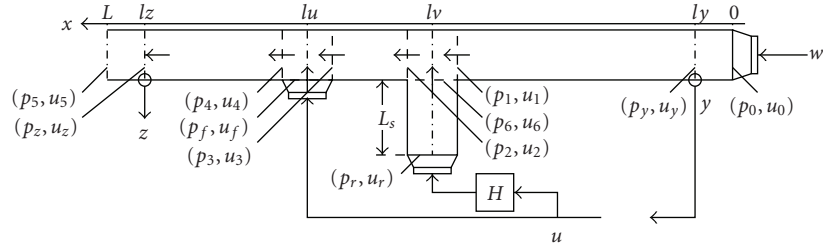

Figure 2: Model for $G(s)$ with a generalized control source.

In the following, only a derivation process of $\widetilde{G}_{yu}$ will be explained ($(j\omega)$ will be omitted). The other 3 transfer functions can be similarly derived.

It is assumed as a boundary condition that $p_5 = 0$ holds at the open-end, and $u_0 = 0$ at the closed-end. In addition, the width of the loudspeaker is assumed to be sufficiently small. It is also assumed that there is no dissipation in sound propagation. Then, the following relationships are obtained by using the transfer matrix method [9] by which a pair of complex pressure and particle velocity at a certain location in the duct is described as a pair at different location with distance l multiplied by a transfer matrix $T(l)$ as below:

$$\begin{bmatrix} p_1 \\ u_1 \end{bmatrix} = T(l_v)\begin{bmatrix} p_0 \\ 0 \end{bmatrix}, \qquad \begin{bmatrix} p_3 \\ u_3 \end{bmatrix} = T(l_u - l_v)\begin{bmatrix} p_2 \\ u_2 \end{bmatrix}, \tag{1}$$

$$\begin{bmatrix} 0 \\ u_5 \end{bmatrix} = T(L - l_u)\begin{bmatrix} p_4 \\ u_4 \end{bmatrix}, \qquad \begin{bmatrix} p_6 \\ u_6 \end{bmatrix} = T(L_S)\begin{bmatrix} p_r \\ u_r \end{bmatrix}, \tag{2}$$

$$T(l) := \begin{bmatrix} \cos kl & -j\rho_0 c_0 \sin kl \\ -\dfrac{j}{\rho_0 c_0}\sin kl & \cos kl \end{bmatrix}, \quad k := \frac{\omega}{c_0}, \tag{3}$$

where ρ_0 is the density of the medium. Moreover, the following standard assumptions are posed:

$$\begin{aligned} &p_1 = p_2 = p_6, \qquad p_4 = p_3 = p_f, \\ &u_2 = u_1 + u_6, \qquad u_4 = u_3 + u_f, \qquad u_r = Hu_f. \end{aligned} \tag{4}$$

Then, the following equality holds:

$$\begin{aligned} \begin{bmatrix} 0 \\ u_5 \end{bmatrix} &= T(L - l_u)\begin{bmatrix} p_4 \\ u_4 \end{bmatrix} \\ &= T(L)\begin{bmatrix} p_0 \\ 0 \end{bmatrix} + T(L - l_v)\begin{bmatrix} 0 \\ u_6 \end{bmatrix} + T(L - l_u)\begin{bmatrix} 0 \\ u_f \end{bmatrix}, \end{aligned} \tag{5}$$

where the relation $T(l_1)T(l_2) = T(l_1 + l_2)$ is used. After eliminating intermediate variables such as u_6, p_r, and u_r by using above relationships, $\widetilde{G}_{yu}$ is obtained as shown in (6) in the next page. The other functions are shown in (7)–(9):

$$\widetilde{G}_{yu} = \frac{p_y}{u_f} = \cos kl_y \cdot \widetilde{G}_{0u},$$

$$\widetilde{G}_{0u} := \frac{p_0}{u_f} = j\rho_0 c_0 \frac{\sin k(L - l_v)H + \sin k(L - l_u)\cos kL_S}{\cos kL \cos kL_S - \sin k(L - l_v)\sin kL_S \cos kl_v}, \tag{6}$$

$$\begin{aligned} \widetilde{G}_{zu} = &\left(\cos kl_z - \frac{\sin k(l_z - l_v)\sin kL_S \cos kl_v}{\cos kL_S}\right)\widetilde{G}_{0u} \\ &- j\rho_0 c_0\left(\sin k(l_z - l_u) + \frac{\sin k(l_z - l_v)\cdot H}{\cos kL_S}\right), \end{aligned} \tag{7}$$

$$\widetilde{G}_{yw} = \cos kl_y \cdot \widetilde{G}_{0w} - j\rho_0 c_0 \sin kl_y,$$

$$\widetilde{G}_{0w} := j\rho_0 c_0 \frac{\sin kL \cos kL_S - \sin k(L - l_v)\sin kL_S \sin kl_v}{\cos kL \cos kL_S - \sin k(L - l_v)\sin kL_S \cos kl_v}, \tag{8}$$

$$\begin{aligned} \widetilde{G}_{zw} = &\left(\cos kl_z - \frac{\sin k(l_z - l_v)\sin kL_S \cos kl_v}{\cos kL_S}\right)\widetilde{G}_{0w} \\ &- j\rho_0 c_0\left(\sin kl_z + \frac{\sin k(l_z - l_v)\sin kL_S \sin kl_v}{\cos kL_S}\right). \end{aligned} \tag{9}$$

It can be easily checked that (6)–(9) is consistent with results in [5] for cases (a) and (b) by substituting $L_S = 0$, $H(j\omega) = 0$, or $H(j\omega) = -e^{-j\omega((l_u - l_v)/c_0)}$.

Note that $H(s)$ is only appeared in $\widetilde{G}_{yu}(s)$ and $\widetilde{G}_{zu}(s)$ since the corresponding control source is operated by u. Furthermore, the open-loop frequency response function

Table 1: Experimental instruments.

Loudspeaker (SPK1-3)	FOSTEX FE87E
Microphones	Electret condenser type
Power amplifier	TOSHIBA TA8213K
LPF for measurements	NF ELECTRONIC INSTRUMENTS FV-664 (2 ch, 200 Hz, 24 dB/oct)
LPF for driving	500 Hz 4th order Butterworth
PC	Dell PowerEdge840 (RTAI3.6.1/Linux kernel 2.6.20.21)
A/D, D/A	CONTEC AD12-16(PCI), DA12-4(PCI) (12 bit, ± 5 V, 10 μs)

$\widetilde{G}_{zw}(s)$ for cases (a) and (b) is common since $L_S = 0$ in both cases. The situation is similar for $\widetilde{G}_{yw}(s)$.

Note that there are two major differences between the experimental ducts and the first principle model: (i) damping or dissipation effect and (ii) number of loudspeakers in case (c). For (i), the experimental duct system might have large damping effect due to the flexible PVC ducts, while the first principle model does not depend on damping effect. For (ii), the front and rear sound from SPK2 in the experimental apparatus are modeled by using two loudspeakers in the first principle model. These points will be discussed in the next section.

4. Comparison of First Principle Model and Experimental Results

Figure 3 shows frequency responses of experimental results and the first principle model.

For the first principle model, the following parameters are used from the configuration of the experimental apparatus in Figure 1: $L = 3.61$, $l_y = 0.03$, $l_v = 1.61$, $l_u = 2.32$, and $l_z = 3.53$. The parameter L_S and H are set as explained in the previous section for each control source. In addition, $c_0 = 344$, $\rho_0 = 1.21$ are used. We also assume $k = \omega/c_0 - 0.09j$ instead of (3) in order to consider the dissipation as in [10], which implies that the first principle model $\widetilde{G}(s)$ is evaluated on a slightly-shifted imaginary axis by setting $s = jkc_0 = j\omega + 30$ where the value 30 was chosen for a better comparison with the experimental result. Furthermore, gain characteristics of the first principle model is divided by 1000 just convenience of comparison to experimental result using the same scales of figures. Note that the gain characteristics calculated by the first principle model do not roll off in the high frequency range, since the low pass filters are neglected in the model as mentioned in the previous section.

It can be seen that the first principle models are consistent with the frequency response experiments in the cases (a) and (b). The gain characteristics of G_{zw} and G_{yw} have peaks at about 24, 71, 119, 167, 214, and 262 Hz which are resonance frequencies given by $f_i := (2i-1)c_0/4L$ $(i = 1, 2, \ldots)$. In gain characteristic of G_{zu}, the gain of case (a) is lower than that of case (b) at the frequency ranges between f_1 and f_2, f_2, and f_3, and so on, while it is higher at the frequency range below f_1. In gain characteristic of G_{yu}, the gain of case (a) has a notch at the frequency range between f_3 and f_4. For phase characteristic of G_{yu}, the phase-lag of case (b) is consistent with a delay element $-e^{-s(2(L-l_u)/c_0)}$. Indeed it is similar to the broken curve in magenta, which is obtained by adding the delay to the original characteristic of case (a). Note that this fact has been already pointed out for the first principle model [5]. Because of the consistencies between the frequency responses of the experimental result and the first principle model, one might conclude that the damping effect due to the flexible PVC duct is not important to affect the comparison result.

In addition to the cases (a) and (b), the first principle model also matches to the experimental results in the case (c). For example, the gain characteristics of G_{zw} and G_{yw} has a deep around f_3 compared with those of cases (a) and (b).

The purpose of the proposed method is to provide an alternative method putting an additional phase-lag against the case (a). In the experiment, it can be seen that the phase characteristic of case (c) is similar to that of the case (b) in the middle frequency range, which justifies to use the proposed source for an inexpensive ANC system. However the phase-lag is not large in the first principle model. The reason is under consideration, but we may conclude that a proper setting of H makes the phase-lag larger. In the phase characteristic of the first principle model $\widetilde{G}_{yu}$ in Figure 3, the broken curve of magenta shows that for $H = -0.95$ instead $H = -1$, where a larger phase-lag appears. This might be consistent to the experimental result since the rear sound could be smaller than the front one due to some obstacle of the rear side of the loudspeaker. Therefore, we expect that the proposed source has a similar advantage to the Swinbanks' source. It should be noted here that the gain of G_{zw} and $\widetilde{G}_{zw}$ for case (c) is smaller than those of cases (a) and (b). This implies an advantage of attaching subduct.

The effect of the proposed source on control performance will be examined by control experiments in the next section.

5. Controller Design and Control Experiments

In this section, only outline of the design procedure is explained since the design procedure is the same as in [2]. First, for each control source, a nominal plant is obtained by the subspace-based method from the frequency response experiment results shown in left-hand side of Figure 3, where the order is taken as 53. Secondly, in order to guarantee the closed-loop stability against the modeling error of the nominal plant, an additive uncertainty model is introduced for feedback-path transfer function, $G_{yu}(s)$ as

$$G_{yu}(s) = \overline{G}_{yu}(s) + W(s)\delta(s), \tag{10}$$

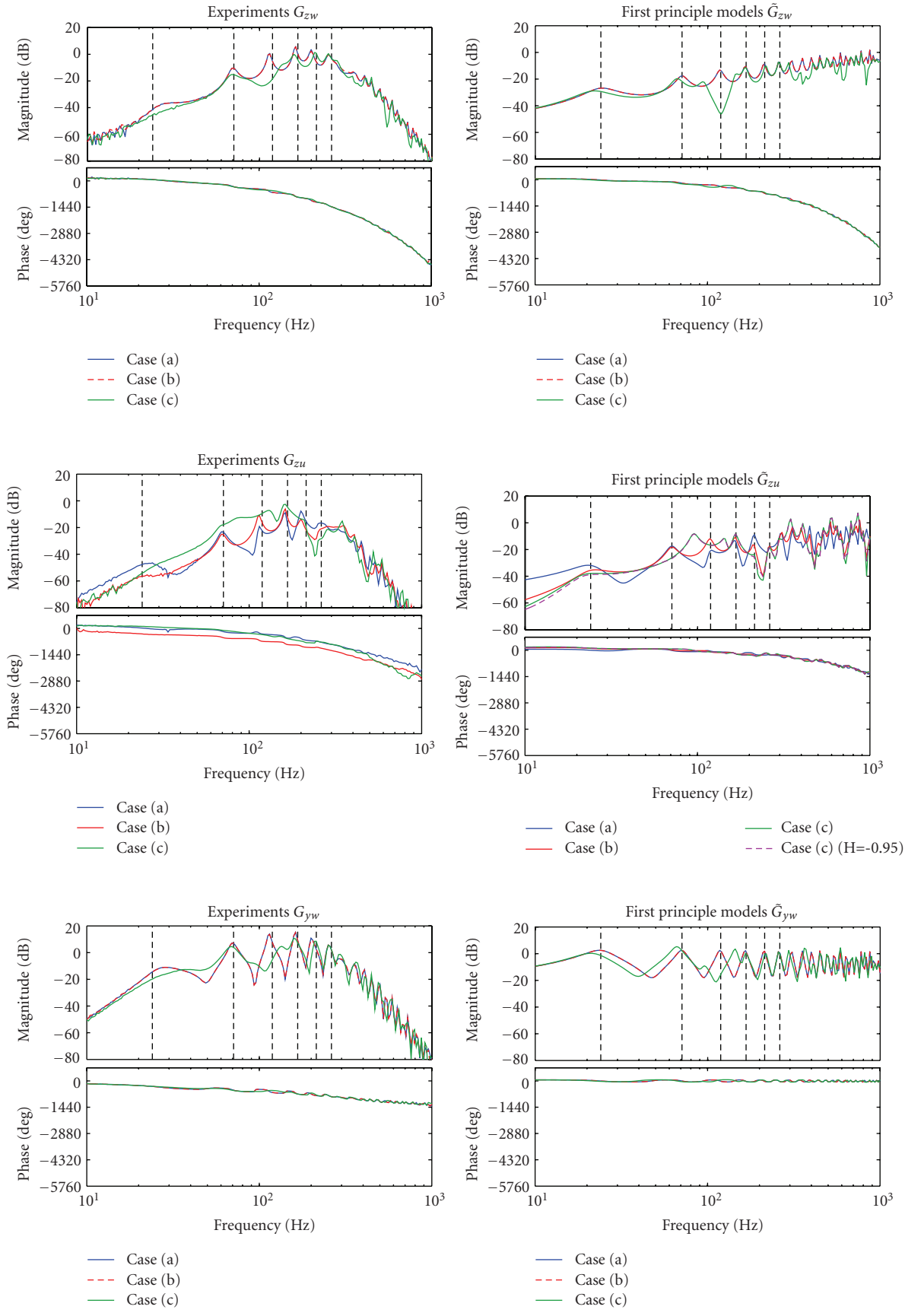

Figure 3: Continued.

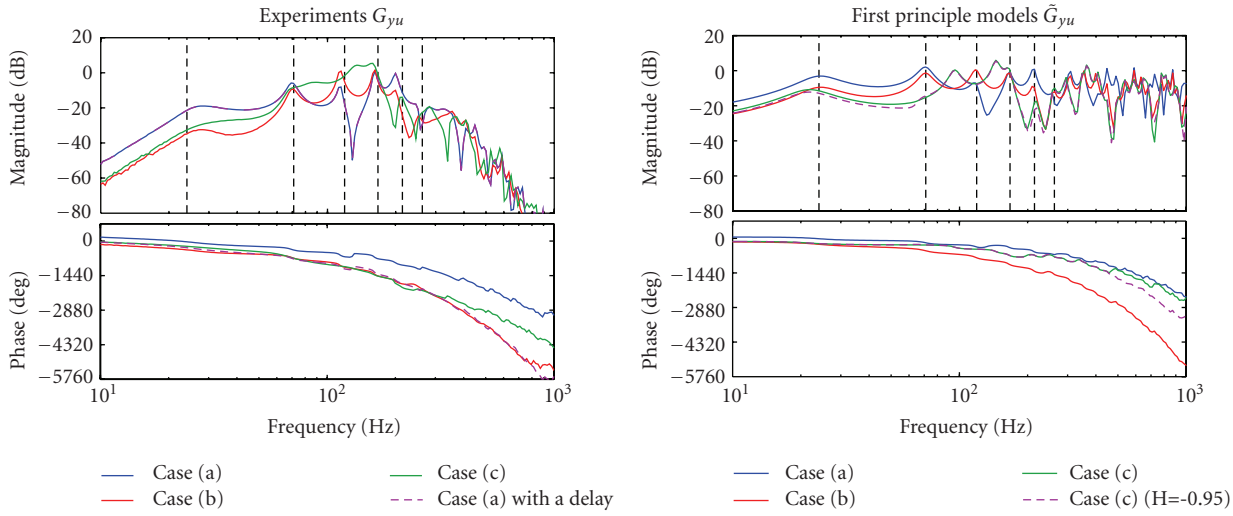

Figure 3: Frequency response experiment G and first principle model $\tilde{G}$.

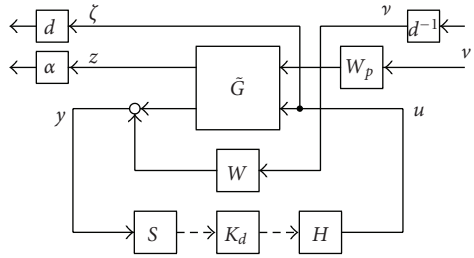

Figure 4: Robust performance problem with scalings.

where $\overline{G}_{yu}(s)$ is the nominal plant for $G_{yu}(s)$, $\delta(s)$ is the normalized modeling error whose $\mathcal{H}_\infty$ norm is less than or equal to 1, and $W(s)$ is a weighting function which is chosen so that G_{yu} can be recovered by δ. We take the common weighting function for all cases as

$$W(s) = 0.06\frac{\omega_1^2}{s^2 + 2\zeta\omega_1 s + \omega_1^2}, \qquad \omega_1 = 2500, \quad \zeta = 0.7. \tag{11}$$

Then, sampled-data $\mathcal{H}_\infty$ control synthesis [11] is applied to the following digital controller design problem: find a discrete-time controller $K_d(z)$ which maximizes the positive scalar α so that the following conditions hold: (i) the closed-loop system of Figure 4 is internally stable; (ii) there exists a positive scalar d such that the L_2 induced norm of the closed-loop system is less than 1, where S is the sampler with sampling period $h = 1$ ms, H is the zero-th order hold, and $W_p(s)$ is a bandpass filter given by

$$W_p(s) = \left(\frac{s}{s+\omega_{p_1}}\right)^2\left(\frac{\omega_{p_2}}{s+\omega_{p_2}}\right)^2, \tag{12}$$

$$\omega_{p_1} = 2\pi \times 40, \quad \omega_{p_2} = 2\pi \times 200.$$

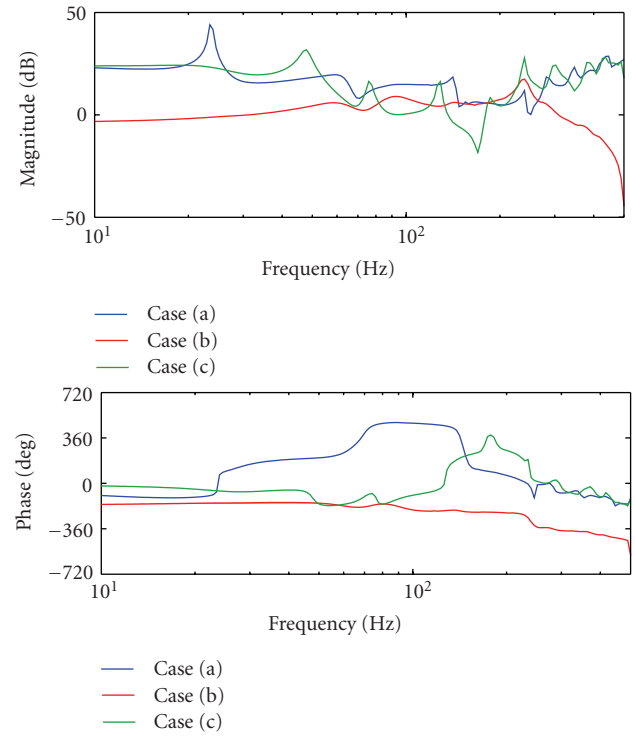

Figure 5: Bode plot of controllers.

Note that the closed-loop system gain is robustly minimized by maximizing α to improve the control performance in the pass band to attenuate the noise.

Figure 5 shows the resultant controller characteristics. It can be seen that the controller of case (b) has the flat gain characteristic in the effective frequency range of the Swinbanks' source, which is consistent with [2]. On the other hand, gain of the cases (a) and (c) have some peaks in the frequency range, however, we expect similar behavior for case

Table 2: Mean square value of error mic. signal $z(t)$.

	Mean square value (V^2)		
	case (a)	case (b)	case (c)
Without cont. (1)	0.00598	0.00575	0.00431
With control (2)	0.00322	0.00166	0.00229
Reduction (1)-(2)	0.00276	0.00409	0.00203

(c) as case (b), since the gain in the middle frequency range is low.

Figure 6 shows time responses of the error microphone signal z, where the first 12.5 seconds is without control and the following 12.5 seconds is with control. The disturbance signal $w(t)$ was generated as a 0-mean uniformly distributed pseudo-random sequence in $[-0.3, 0.3]$ by using `rand()` function in the GNU C Library. The sampling period used for the measurement is 0.5 ms. It can be seen that the ascending order of the peak-to-peak value is case (b) < case (c) < case (a). Namely, the case (c) achieves a better performance than the case (a) without using multiple loudspeakers as in the case (b) with multiple loudspeakers. This can be also confirmed by evaluating mean square value of the time response as shown in Table 2. Note that the error microphone signal without control of case (c) differs from those of cases (a) and (b) due to attaching the subduct. It is also shown in Table 2. One might think that the performance of case (c) could not better than case (a) since the overall noise reduction by control source loudspeaker in case (c) is smaller than that in case (a) as shown in Table 2. However, we here remark that the case (c) might provide better performance than case (a) since the total noise reduction is better than case (a) by accounting the noise reduction given by attaching the subduct.

Figure 7 shows the power spectral density of the error microphone signal $z(t)$ where the Welch spectral estimator is used with the Hamming window, and the segment length is chosen as 2048 which corresponds to about 1 Hz in frequency resolution since the sampling period for measurement is 0.5 ms. In addition, the result of "without control" for case (a) has been shown in the same figure of the case (c), since we are interested in the total performance of the control source including subduct for case (c). It can be seen by comparing the results for "without control" that noise level is reduced by attaching the subduct in case (c), which consists with the gain characteristics of G_{zw} and $\widetilde{G}_{zw}$ in Figure 3 as explained in the previous section. Furthermore, by comparing the "with control" and "without control (case (a))," it can be seen that there are some amplifications in the low frequency range around 50 to 100 Hz, however, case (c) has the similar advantage to case (b) that the magnitude around 6th resonance (262 Hz) is reduced by control, and amplification at the 2nd resonance (70 Hz) is prevented.

Figure 8 shows time responses of control input u. It can be seen that the ascending order of the peak-to-peak value is case (b) < case (c) < case (a), which also shows an advantage of the proposed method against the bidirectional source.

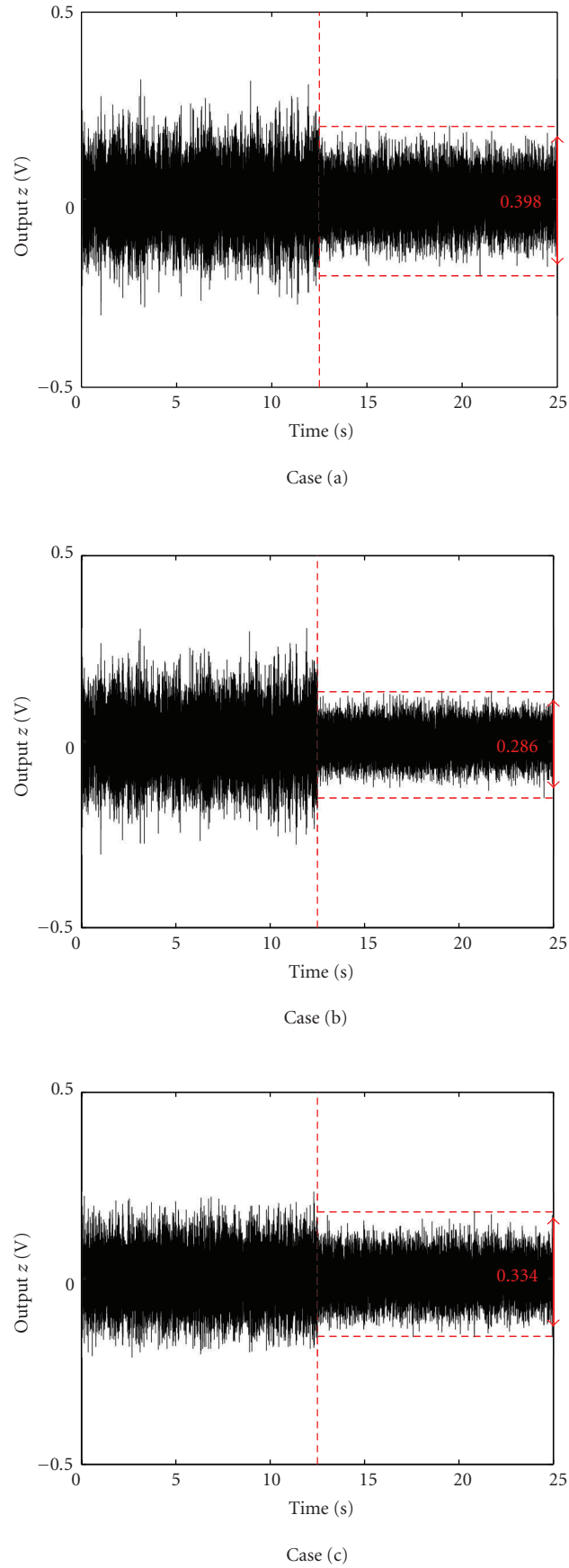

Figure 6: Time response of z.

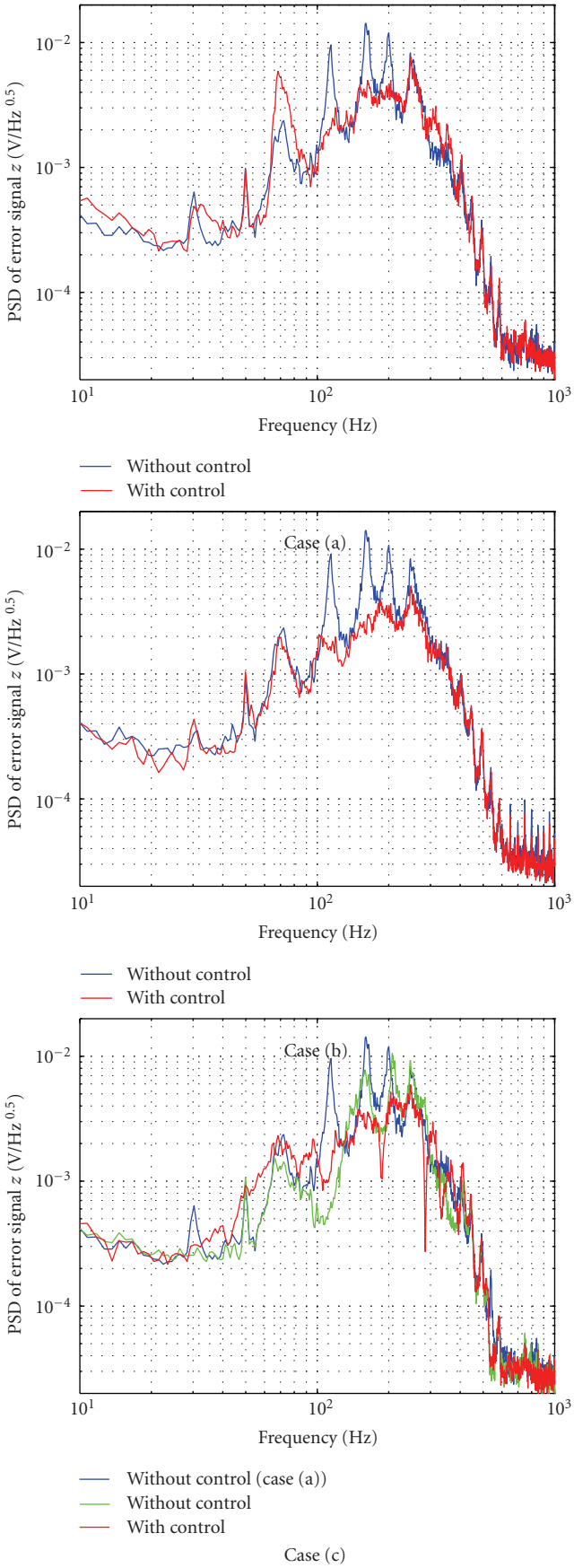

Figure 7: Power spectral density of z.

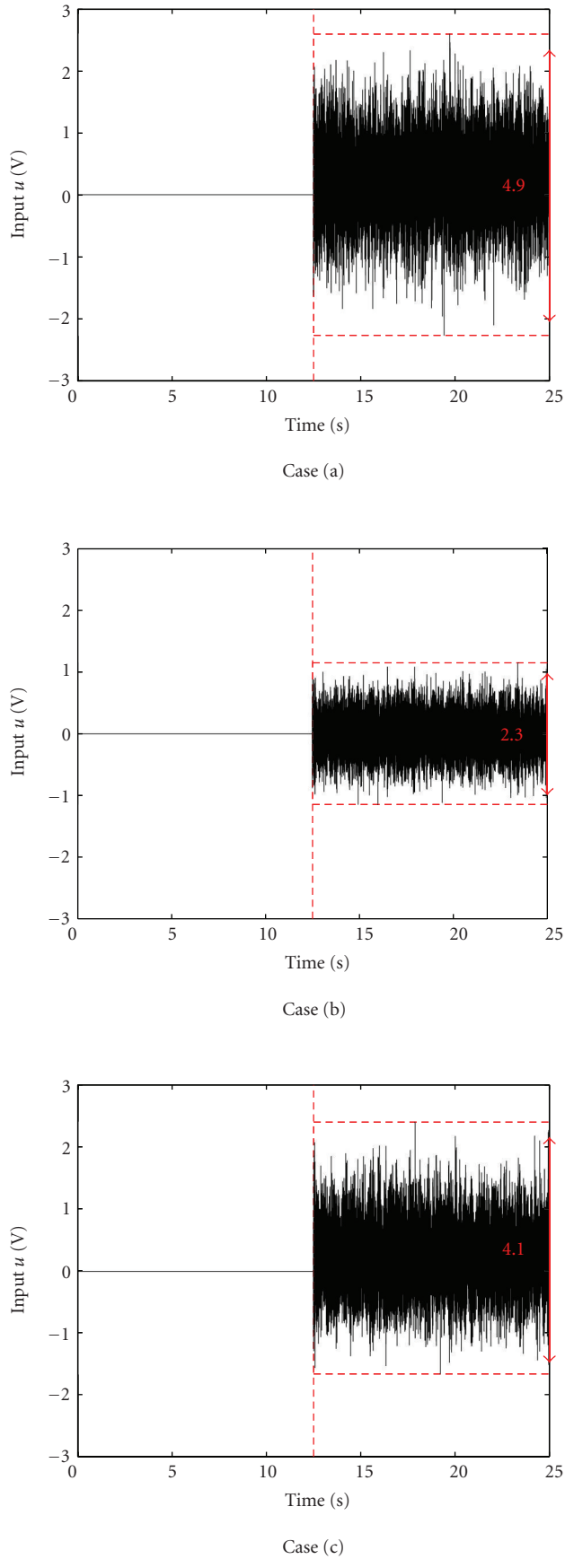

Figure 8: Time response of u.

6. Conclusions

In this paper, a control source which uses the rear sound interference has been proposed for ANC system. The validity of the proposed method has been shown by comparing with the existing bidirectional source and the the Swinbanks' source: three structures of control source have been compared with a simple ducts in open-loop and closed-loop characteristics based on first principle models and experimental results. First, the open-loop transfer function for a generalized control structure unifying the three structures has been derived. Secondly, it has been shown that the open-loop transfer functions are consistent with the frequency response experiments in the cases of bidirectional and the Swinbanks' source. Especially, the additional phase-lag in the feedback path by the Swinbanks' source corresponds to twice of the distance between the control source and the open-end. In the proposed source, a similar phase characteristic as the Swinbanks' source has been shown by frequency response experiments.

Finally, effects on control performances of control source structures have been examined by control experiments with robust controllers. The smaller amplitude in error microphone signal has been achieved with smaller amplitude in driving signal of control source by the proposed source as compared to the bidirectional source. Although the proposed source does not achieve a much better performance than the Swinbanks' source, it has an advantage for inexpensive implementation since less number of loudspeakers are necessary than the Swinbanks' source. There might be a difficult situation to adopt case (c) because of the space limitation on the installation, however, for the situation where the space limitation is mainly on the duct length, the case (c) could be a solution as inexpensive ANC system compared with the case (b) since the distance between the loudspeaker and the upstream junction is the same to the distance between two loudspeakers in case (b).

Therefore we conclude that the proposed structure of control source provides a good trade-off for a well-performed and inexpensive ANC system.

References

[1] M. A. Swinbanks, "The active control of sound propagating in long ducts," *Journal of Sound and Vibration*, vol. 27, pp. 411–436, 1973.

[2] Y. Kobayashi and H. Fujioka, "Active noise cancellation for ventilation ducts using a pair of loudspeakers by sampleddata H_∞ optimization," *Advances in Acoustics and Vibration*, vol. 2008, Article ID 253948, 8 pages, 2008.

[3] S. Kijimoto, H. Tanaka, Y. Kanemitsu, and K. Matsuda, "Howling cancellation for active noise control with two sound sources," *Transactions of the Japan Society of Mechanical Engineers*, vol. 67, no. 656, pp. 52–57, 2001 (Japanese).

[4] J. Winkler and S. J. Elliott, "Adaptive control of broadband sound in ducts using a pair of loudspeakers," *Acustica*, vol. 81, no. 5, pp. 475–488, 1995.

[5] Y. Kobayashi and H. Fujioka, "Analysis for robust active noise control systems of ducts with a pair of loudspeakers," in *Proceedings of the 15th International Congress on Sound and Vibration (ICSV '08)*, Daejeon, South Korea, 2008.

[6] Y. Kobayashi and H. Fujioka, "Robust stability analysis for active noise control systems of ducts with a pair of loudspeakers," in *Proceedings of the 37th Symposium on Control Theory (SICE '08)*, pp. 21–24, 2008.

[7] D. S. Bernstein, "What makes some control problems hard?" *IEEE Control Systems Magazine*, vol. 22, no. 4, pp. 8–19, 2002.

[8] J. Hong and D. S. Bernstein, "Bode integral constraints, colocation, and spilover in active noise and vibration control," *IEEE Transactions on Control Systems Technology*, vol. 6, no. 1, pp. 111–120, 1998.

[9] H. Isaka, K. Nisida, and K. Saito, "Active control of exhaust noise from a muffler in consideration of the location of secondary source," *Transactions of the Japan Society of Mechanical Engineers. C*, vol. 66, no. 645, pp. 1502–1508, 2000 (Japanese).

[10] S. J. Elliott, *Signal Processing for Active Control*, Signal Processing and Its Applications, Academic Press, Boston, Mass, USA, 2000.

[11] T. Chen and B. A. Francis, *Optimal Sampled-Data Control Systems*, Springer, New York, NY, USA, 1996.

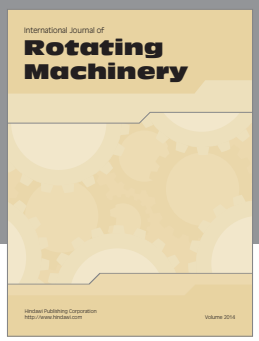

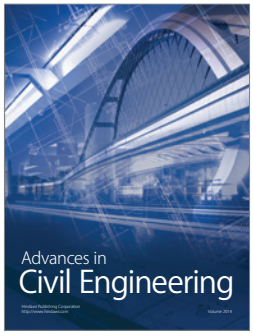

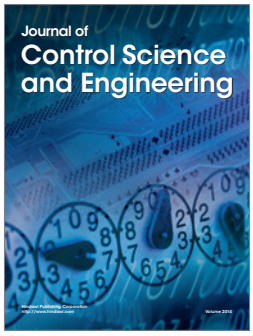

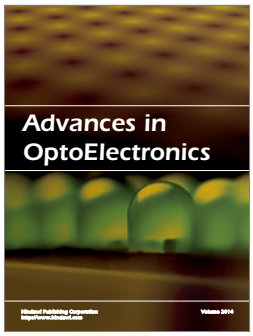

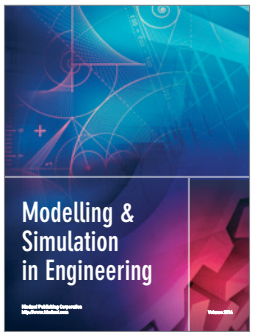

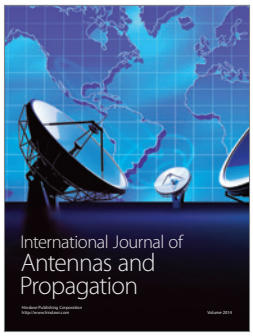

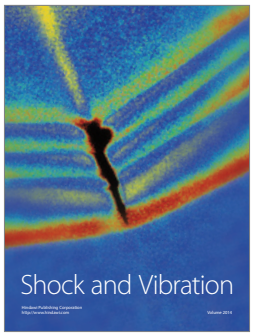

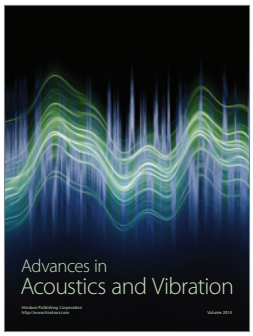

Hindawi

Submit your manuscripts at
http://www.hindawi.com